

Mechanical performances of concrete beams with hybrid usage of steel and FRP tension reinforcement

Linh V. H. Bui^{1a}, Boonchai Stitmannathum^{*1} and Tamon Ueda^{2b}

¹Department of Civil Engineering, Chulalongkorn University, 254 Phayathai Road, Pathumwan, Bangkok 10330, Thailand

²Laboratory of Engineering for Maintenance System, Hokkaido University, Sapporo, Hokkaido Prefecture 060-0808, Japan

(Received February 28, 2017, Revised May 10, 2017, Accepted May 11, 2017)

Abstract. Fiber reinforced polymer (FRP) bars have been recently used to reinforce concrete members in flexure due to their high tensile strength and especially in corrosive environments to improve the durability of concrete structures. However, FRPs have a low modulus of elasticity and a linear elastic behavior up to rupture, thus reinforced concrete (RC) components with such materials would exhibit a less ductility in comparison with steel reinforcement at the similar members. There were several studies showed the behavior of concrete beams with the hybrid combination of steel and FRP longitudinal reinforcement by adopting the experimental and numerical programs. The current study presents a numerical and analytical investigation based on the data of previous researches. Three-dimensional (3D) finite element (FE) models of beams by using ANSYS are built and investigated. In addition, this study also discusses on the design methods for hybrid FRP-steel beams in terms of ultimate moment capacity, load-deflection response, crack width, and ductility. The effects of the reinforcement ratio, concrete compressive strength, arrangement of reinforcement, and the length of FRP bars on the mechanical performance of hybrid beams are considered as a parametric study by means of FE method. The results obtained from this study are compared and verified with the experimental and numerical data of the literature. This study provides insight into the mechanical performances of hybrid FRP-steel RC beams, builds the reliable FE models which can be used to predict the structural behavior of hybrid RC beams, offers a rational design method together with an useful database to evaluate the ductility for concrete beams with the combination of FRP and steel reinforcement, and motivates the further development in the future research by applying parametric study.

Keywords: FRP; hybrid combination; finite element modeling; reinforced concrete

1. Introduction

Nowadays, concrete beams reinforced by steel and fiber reinforced polymer (FRP) bars have been known as the interested topic for the experimental research. The studies of Aiello and Ombres (2002), Qu *et al.* (2009), Lau and Pam (2010), Ge *et al.* (2015) and Yoo *et al.* (2016) have been conducted on deflection, curvature, ductility, crack width of concrete beams with hybrid usage of FRP and steel tension reinforcement. The study by Aiello and Ombres (2002) provides various findings as follows. The hybrid combinations of steel and FRP reinforcement were advantageous in the deformability consideration. The deformability of FRP reinforced concrete (RC) beams under service conditions was reduced by using the adequate amount of steel reinforcement. It was emphasized that placing FRP bars nearly the outer surface and steel bars at the inner level of the tensile zone would increase the stiffness of beams. Moreover, the crack width and spacing

decreased with the presence of steel reinforcement in comparison with the one attained by beams reinforced with only FRP bars. Using the moment-curvature law, the behavior of concrete beams reinforced by steel and FRP bars could accurately predict, and the ACI code furnished a good prediction of the deflections and crack width at the serviceability phase. A design method was proposed to determine the effective moment of inertia for steel RC beams and FRP RC beams based on the calibrated experimental results.

By conducting an experimental and theoretical program, Qu *et al.* (2009) showed that the usage of steel reinforcement in combination with glass fiber reinforced polymer (GFRP) bars enhanced the flexural performance of GFRP RC beams. This research indicated that the axial stiffness ratio between GFRP and steel bars had little influence on flexural capacity, whereas the effective reinforcement ratio was a reasonable parameter for predicting the ultimate moment of hybrid reinforced concrete beams. In order to predict the failure mode of hybrid beams, the balanced effective reinforcement ratio could be used. Their study proposed the flexural capacity equation which was valid for hybrid GFRP-steel RC members by using normal effective reinforcement ratios. The ductility of beams was increased by adding the steel reinforcements. At the service load level, the model of Bischoff (2007) was adopted to calculate the deflection of

*Corresponding author, Associate Professor
E-mail: Boonchai.S@chula.ac.th

^aPh.D. Candidate
E-mail: bvhlinh@gmail.com

^bProfessor

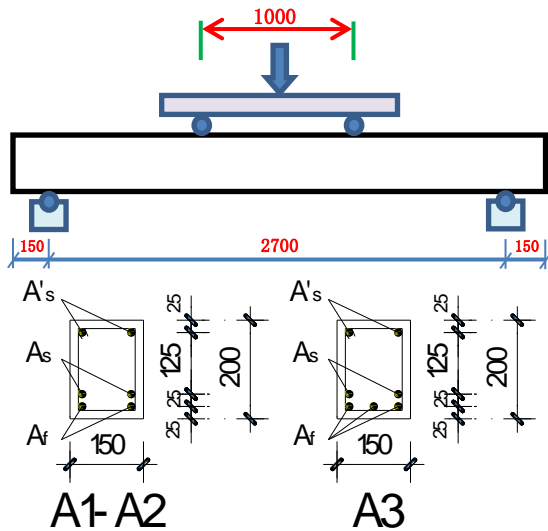


Fig. 1 Geometrical dimension of the tested beams (Aiello and Ombres 2002)

Table 1 The properties of the tested beams (Aiello and Ombres 2002)

Beam group	Beam ID	A_s (mm ²)*	A_f (mm ²)*	$\rho_r = A_f/A_s$
Hybrid beams	A1	100.48 (2d8)	88.36 (2d7.5)	0.8789
	A2	100.48 (2d8)	157.08 (2d10)	1.5625
	A3	226.19 (2d12)	235.62 (3d10)	1.0417

* A_s and A_f : The area of the steel and AFRP tension reinforcement, respectively

concrete beams reinforced with GFRP and steel bars. In another experimental work, Lau and Pam (2010) concluded that increasing the degree of over-reinforcement and adding conventional steel bars could improve the flexural ductility of GFRP RC members. The requirement contents on the minimum GFRP flexural reinforcement given by ACI 440.1R-06 could be reduced by about 25% based on the results of this study.

Ge *et al.* (2015) experimented the flexural behaviors of hybrid concrete beams reinforced with BFRP (basalt fiber reinforced plastic) bars and steel bars. This research used the proposed formula with the measured strengths of bars and concrete to compute the flexural capacity and made the comparison with the experimental results. It was shown that the experimental results had a good agreement with the simplified proposed formula, therefore the suggested equations could be used in future applications. Decreasing the area ratios of BFRP to steel reinforcement, the deflection of hybrid RC beams decreased, whereas the stiffness reduction factor increased. The average crack spacing of the hybrid FRP-steel RC beams was in the middle of the average crack spacing of the steel RC beams and FRP RC beams. In contrast to the above-mentioned studies, Yoo *et al.* (2016) investigated the flexural behavior of ultra-high-performance fiber-reinforced concrete (UHPC) beams reinforced with GFRP and steel bars. And their research showed that the ductility of UHPC beams reinforced by GFRP and steel bars were similar or

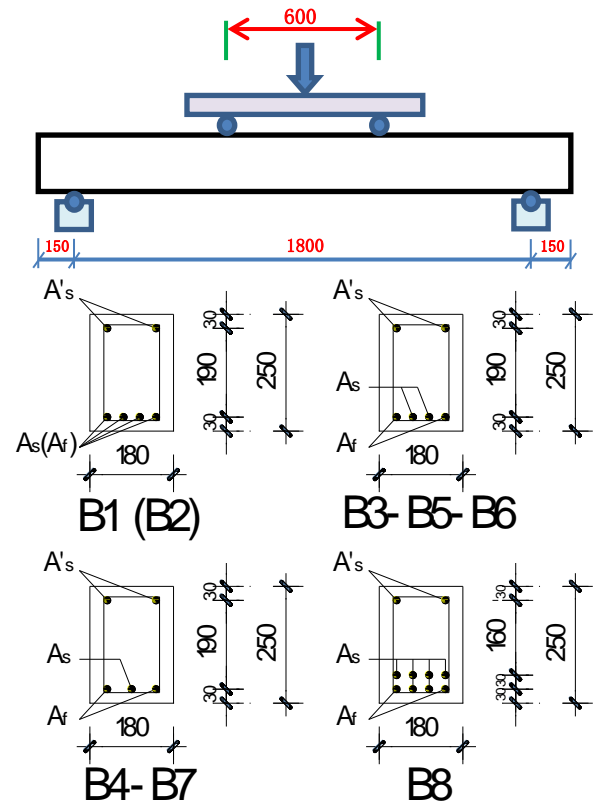


Fig. 2 Geometrical dimension of the tested beams (Qu *et al.* 2009)

Table 2 The properties of the tested beams (Qu *et al.* 2009)

Beam groups	Beam ID	A_s (mm ²)*	A_f (mm ²)*	$\rho_r = A_f/A_s$
Control beams	B1	452.16 (4d12)	-	-
	B2	-	506.45 (4d12.7)	-
Hybrid beams	B3	226.08 (2d12)	253.23 (2d12.7)	1.1201
	B4	200.96 (1d16)	396.91 (2d15.9)	1.9751
	B5	401.92 (2d16)	141.69 (2d9.5)	0.3525
	B6	401.92 (2d16)	253.23 (2d12.7)	0.6301
	B7	113.04 (1d12)	141.69 (2d9.5)	1.2535
	B8	1205.76 (6d16)	396.91 (2d15.9)	0.3292

* A_s and A_f : The area of the steel and GFRP tension reinforcement, respectively

slightly less than those of single GFRP bar-UHPFRC beams due to the premature rupture of steel reinforcement.

Up to now, there were several researches on the numerical analysis of the hybrid FRP-steel RC beams as Kara *et al.* (2015, 2016), Hawileh (2015), Oller *et al.* (2015), Yoo and Banthia (2015), Bencardino *et al.* (2016), Zhang *et al.* (2016) and Qin *et al.* (2017). These studies used the numerical method for estimating the curvature, deflection and moment capacity of hybrid FRP-steel RC beams. And the ductility definitions were also suggested in those papers. Most studies showed a good agreement in the comparison between the numerical and experimental results. However, the numerical studies based on FE model were limited to 2D analysis. Besides, the FE analysis

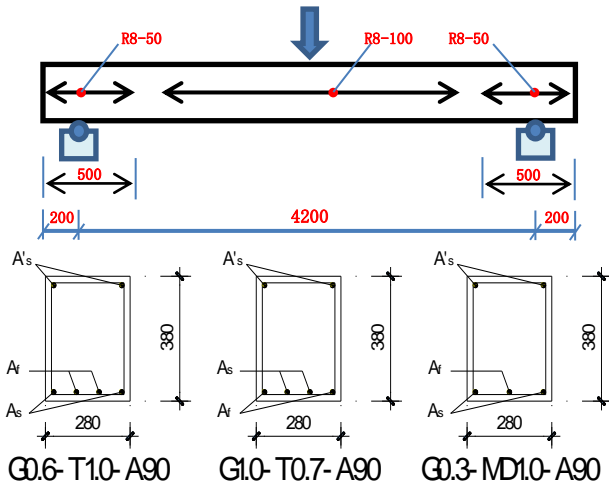


Fig. 3 Geometrical dimension of the group tested beams (Lau and Pam 2010)

Table 3 The properties of the tested beams (Lau and Pam 2010)

Beam group	Beam ID	A_s (mm ²)*	A_f (mm ²)*	$\rho_r = A_f/A_s$
	G0.6-T1.0-A90**	981.75 (2T25)	567.06 (2G19)	0.5776
Hybrid beams	G1.0-T0.7-A90**	628.32 (2T20)	981.75 (2G25)	1.5625
	G0.3-MD1.0-A90**	981.75 (2MD25)	283.53 (1G19)	0.2888

* A_s and A_f : The area of the steel and GFRP tension reinforcement, respectively

**MD, T, G, and A90: The mild steel, high yield steel, GFRP reinforcement, and 90° hook angle in stirrups, respectively

studies employed a little experimental data from the literature, thus the outcome of simulation did not gain the high reliability. Furthermore, the deflection evaluation by the existing method and code were not good enough for predicting the midspan displacement of hybrid beams. Therefore, additional numerical and analytical investigation are necessary.

The primary objective of this study is to understand the mechanical behavior of hybrid FRP-steel RC beams for orienting the practical application to develop rational design method. Three-dimensional (3D) finite element (FE) models using ANSYS 15.0 have been developed to simulate the performance of concrete beams in the literature of Aiello and Ombres (2002), Qu *et al.* (2009), Lau and Pam (2010). Furthermore, FE models have been implemented to investigate the effects of reinforcement ratio, concrete compressive strength, arrangement of tension reinforcement, and the length of FRP bars on the flexural response of hybrid FRP-steel RC beams. In addition, the design methods in terms of moment capacity, load-deflection relations, crack width prediction and ductility of hybrid FRP-steel RC beams were discussed and proposed. Moreover, the useful database to assess the ductility of hybrid beams were presented. The further studies are expected through the parametric study.

2. Experimental data

Table 4 The mechanical properties of materials

Study	Beam ID	f_c (MPa)	f_t (MPa)	f_f (MPa)	E_f (MPa)	ρ_s (%)	ρ_f (%)
Aiello and Ombres (2002)	A1	38	558	1674	49000	0.335	0.294
	A2	38	558	1366	50100	0.335	0.523
	A3	38	558	1366	50100	0.754	0.785
Qu <i>et al.</i> (2009)	B1	30.95	363	NA	NA	1.142	NA
	B2		NA	782	45000	NA	1.280
	B3	33.10	363	782	45000	0.571	0.640
	B4		336	755	41000	0.508	1.003
	B5	34.40	336	778	37700	1.015	0.358
	B6		336	782	45000	1.015	0.640
	B7	40.65	363	778	37700	0.286	0.358
	B8		336	755	41000	3.269	1.076
Lau and Pam (2010)	G0.6-T1.0-A90	44.6	550	588	39500	0.923	0.533
	G1.0-T0.7-A90	39.8	597	582	38000	0.591	0.923
	G0.3-MD1.0-A90	41.3	336	588	39500	0.923	0.266

The data in the experimental program of Aiello and Ombres (2002), Qu *et al.* (2009), Lau and Pam (2010) were adopted to verify the FE models. The following experimental studies have been described.

Aiello and Ombres (2002) presented an experimental investigation of five concrete beams (150×200×3000 mm) reinforced by hybrid usage of aramid fiber-reinforced polymer (AFRP) and steel reinforcement. One beam was reinforced by only AFRP bars, another one was reinforced with only steel reinforcement, and three hybrid AFRP-steel reinforced concrete beams. Four-point flexural loading tests were conducted on the beams. All beams used the two steel bars of 8 mm diameter as the compression reinforcement, and transverse reinforcement of 8 mm diameter and 100 mm spacing were employed as shear reinforcement. More details of the selected beams investigated for the current study are shown in Fig. 1 and Table 1.

Qu *et al.* (2009) studied the flexural behavior of concrete beams reinforced with hybrid (GFRP and steel) bars. This research employed eight concrete beams (180×250×1800 mm), including two control beams reinforced with only steel or only GFRP bars, and six hybrid FRP-steel RC beams. All beams used the two steel bars of 10 mm diameter as the compression reinforcement and steel stirrups with 10 mm diameter and 100 mm spacing as shear reinforcement. A four-point flexural loading test was conducted. More details of the specimens are found in Fig. 2 and Table 2.

Lau and Pam (2010) studied on the twelve specimens, simply supported and subjected to a point load at midspan, including plain concrete beams, steel-reinforced concrete (SRC) beams, pure GFRP RC beams, and hybrid GFRP-steel RC beams. The objectives of this study were to understand the flexural behavior of GFRP RC beams and to provide guidelines on the ductility improvement of GFRP RC beams. The two steel bars of 6 mm diameter were employed as the compression reinforcement, steel stirrups with 8 mm diameter and 50 mm spacing at the two ends of

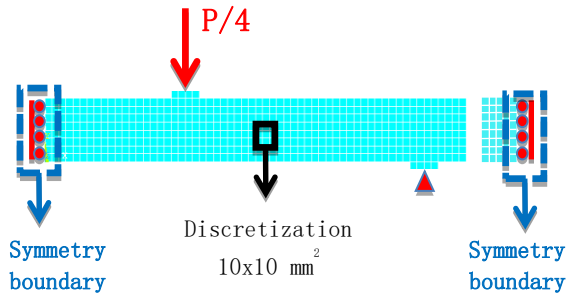


Fig. 4 A quarter typical FE model for numerical program by using ANSYS 15.0

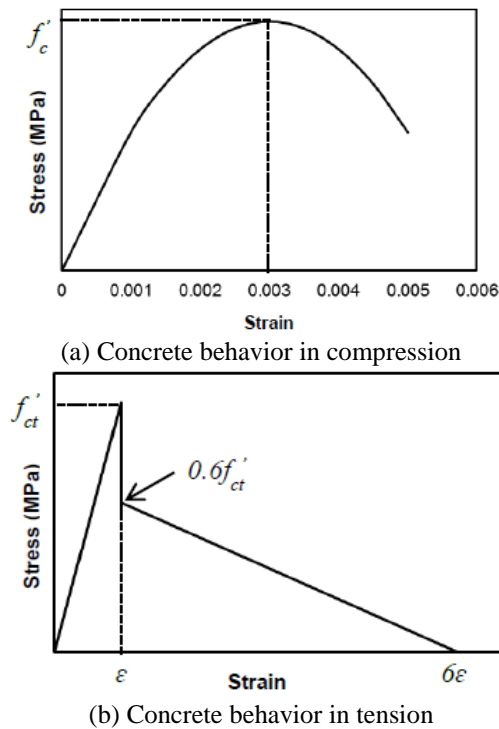


Fig. 5 Models of concrete in compression and tension

beams and 100 mm spacing at the rest of beams were applied as shear reinforcement. Fig. 3 and Table 3 show the more details of the beam specimens which are investigated in the present study.

The mechanical properties of concrete, steel, and FRP reinforcement of all the investigated beams taken from the above three past studies are shown in Table 4. Where, for each study are indicated: beam ID, concrete compressive strength (f'_c), steel yielding strength (f_y), ultimate strength and elastic modulus of FRP reinforcement (f_f , E_f), reinforcement content of steel and FRP bars are ρ_s and ρ_f , respectively.

3. Three-dimensional (3D) finite element (FE) analysis

3.1 Finite element program

In this study, numerical analyses were conducted by a

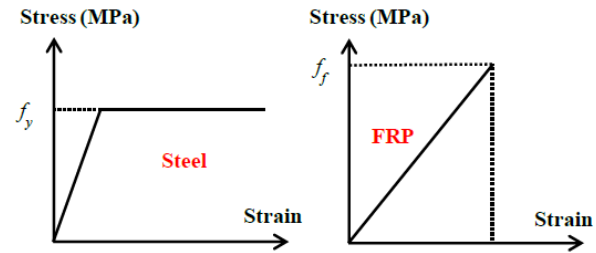


Fig. 6 Stress-strain relationships of steel and FRP reinforcement

commercially available software, ANSYS 15.0. A quarter FE model was applied to investigate the performance of the tested beams based on the symmetric condition as shown in Fig. 4. For this investigation, the mesh discretization is the $10 \times 10 \text{ mm}^2$.

3.1.1 Element types

SOLID65 is used for the nonlinear 3D modeling of concrete materials. The SOLID65 element is capable of cracking in tension and crushing in compression. The element is defined by eight nodes and at each node has three degrees of freedom that are the translations in the nodal x, y, and z directions. LINK180 element is assigned for the steel and FRP reinforcement. LINK180 is a uniaxial tension-compression element with three degrees of freedom at each node that the translations in the nodal x, y, and z directions. The loading and rigid steel supports are modeled by employing SOLID45. The SOLID45 has the same properties as that of SOLID65 except for the capability of cracking in tension and crushing in compression (Hawileh 2015). The perfect bond behavior between FRP and concrete is assumed in the FE models.

3.1.2 Material models

Various constitutive models have been employed in FE simulations of hybrid FRP-steel RC beams to describe the behavior of concrete under a wide range of complex stress and strain histories. These models included nonlinear elastic models, plasticity based models whether perfect plasticity models or elastic-plastic models (Godat *et al.* 2012). In this study and Hawileh (2015), Hind *et al.* (2016), the model of Hognestad *et al.* (1955) is adopted to simulate the nonlinear response of concrete in compression. Eq. (1) and Fig. 5(a) show the more details of Hognestad *et al.* (1955) model.

$$f_c = f'_c \left[2 \left(\frac{\varepsilon}{\varepsilon_0} \right) - \left(\frac{\varepsilon}{\varepsilon_0} \right)^2 \right] \quad (1)$$

Where

f_c is the compressive stress of concrete (MPa) corresponding to the specified strain, ε ,

f'_c is the concrete compressive strength (MPa),

$\varepsilon_0 = \frac{2f'_c}{E_c}$, and E_c is the elastic modulus of concrete

(MPa).

The concrete behavior in tension according to the model of William and Warnke is recommended by ANSYS, and

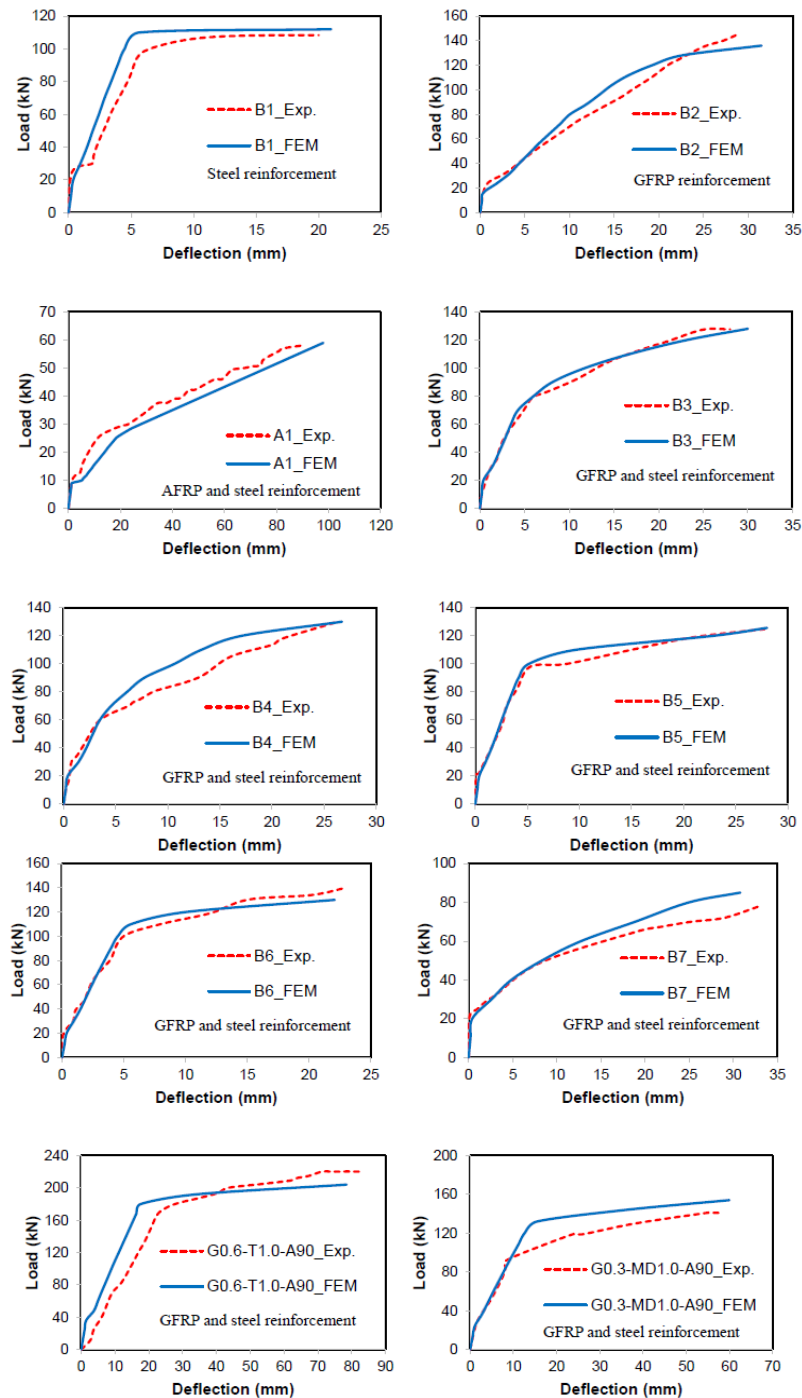


Fig. 7 Comparison of load-midspan deflection relationship between the tested and FE results: The first two specimens are steel and FRP RC beams, respectively, and the remaining specimens are hybrid beams

Fig. 5(b) shows the stress-strain relationship of concrete in tension. The linear elasticity to the concrete tensile strength is used for concrete behavior in tension. Then, a step drop in the concrete tensile stress by 40% is the stress relaxation in tension. And the rest of model is represented as the curve which descends linearly to zero tensile stress at a strain value 6 times larger than strain value at the concrete's tensile strength (Hawileh 2015). Besides, the steel reinforcement is described as the elastic fully plastic model based on the von Mises yield criterion, while the FRP bars are simulated as elastic-brittle materials till rupture. Fig. 6

shows the stress-strain relationships of steel and FRP reinforcement which are applied in the FE analysis.

3.2 Results and discussion

The concrete beams reinforced by steel, FRP, and steel-FRP bars are simulated and the simulation results are investigated. The failure definition of beam specimens in the FE analysis is either the concrete compressive strain exceeding 0.003 or the stress in FRP reinforcement reaching their tensile strength. The predicted load-midspan deflection

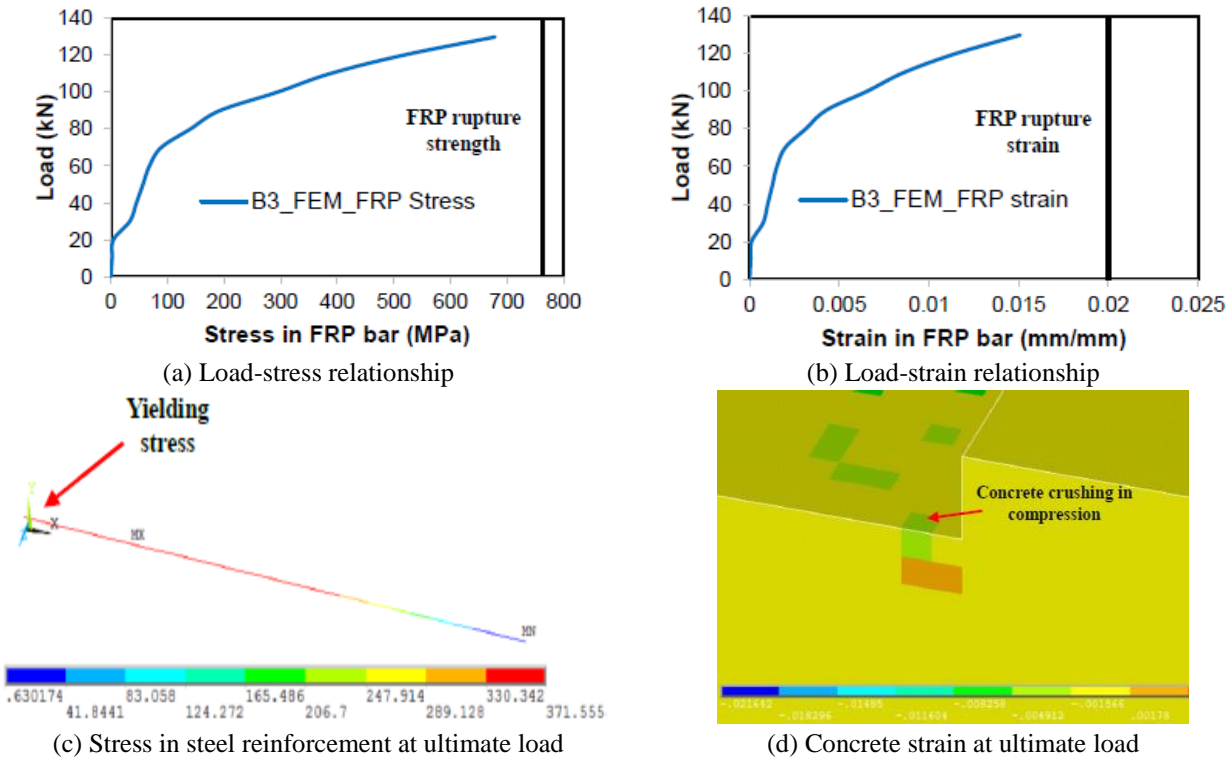


Fig. 8 Load-stress, load-strain relationships in FRP bar, stress of steel reinforcement, and concrete strain at ultimate load of the representative hybrid beam B3

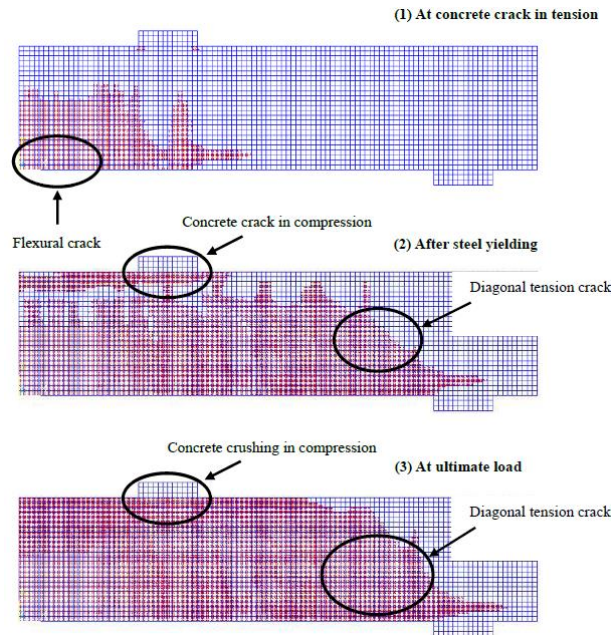


Fig. 9 Crack propagation under the load stages of the representative hybrid FRP-steel RC beam B3

response, failure modes of the developed models are compared with the results obtained from the corresponding experimental data. Moreover, the structural performances of the hybrid FRP-steel RC beams in terms of load-stress, load-strain relationships of FRP bars, and crack propagation at the load steps are also discussed.

Fig. 7 shows the load-midspan deflection curves of experimental and simulated results for the ten beam specimens with the one steel RC beam, one pure FRP RC

beam, and eight hybrid FRP-steel RC beams. It is explicit that the FE results perform the good appraisal in the comparison with the tested data, and a maximum deviation less than 10% not only in the load-carrying capacity but also in the displacement is easily found from Fig. 7 and Table 5. In general, the load-displacement curves from the FE analysis are slightly stiffer than those from the experimental results due to the perfect bond assumption between reinforcement and concrete in the FE model may

Table 5 Experimental and numerical results for load capacity and failure mode

Authors	Beam ID	P _{exp.} (kN)	P _{num.} (kN)	Difference (%)	Failure mode		
					Experiment	Simulation	
Aiello and Ombres (2002)	A1	58	59	1.72	SY-CC*	SY-CC	
	B1	108	112	3.70	SY-CC	SY-CC	
	B2	145	136	6.21	SY-CC	SY-CC	
	B3	127	128	0.79	SY-CC	SY-CC	
	Qu <i>et al.</i> (2009)	B4	129	130	0.78	SY-CC	SY-CC
		B5	125	125	0.00	SY-CC	SY-CC
		B6	140	130	7.14	SY-CC	SY-CC
Lau and Pam (2010)	B7	78	85	8.97	SY-CC	SY-CC	
	G0.6-T1.0-A90	220	204	7.27	SY-CC	SY-CC	
	G0.3-MD1.0-A90	141	154	9.22	SY-CC	SY-CC	

*SY and CC: The steel yielding and concrete crushing, respectively

unreasonable for simulating the real structures. Besides, the effects of the concrete shrinkage, which may cause cracking, are not considered in the simulation. This fact can be another cause for this overestimated stiffness. On the other hand, by using FRP bars, the load capacity of the hybrid beam increases and the overall beam behavior changes to be more brittle.

As shown in Table 5, the simulated beams are failed in the concrete crushing after steel yielding and this failure mode was also indicated in the experimental program of the literature. An evidence for this statement is proved from Figs. 8(a)-(b), the stress and strain of FRP bar in the beam B3 are less than the rupture values, whereas at the similarly ultimate load, the steel reinforcement is yielded (Fig. 8(c)) and the concrete is crushed (Fig. 8(d) and Fig. 9). Furthermore, the crack propagation at the applied load stages of concrete beams with the hybrid usage of FRP and steel reinforcement are exhibited in Fig. 9. At first, the flexural cracks appear vertically at the bottom of the midspan of beams when a principal tensile stress exceeds the ultimate tensile strength of the concrete material. With the increase of load, the cracking region propagated horizontally to the support positions and the diagonal tension cracks are formed, which is followed by the yielding of steel reinforcement. The stiffness of the beam at this stage depends on the elastic modulus of FRP. The additional diagonal, and flexural cracks as well as the concrete cracks in compression are induced as increasing the load level. Finally, the concrete crushing in the compressive zone is recognized as the failure mode of the investigated hybrid RC beams.

The general response of concrete beams with the hybrid usage of steel and FRP reinforcement is further discussed in section 5.3 for studying the design models. In concluding, the FE method is an effective tool to accurately predict various features, including the load-midspan deflection, load-strain/stress responses, failure mode, and crack propagation of concrete beams reinforced with the steel, pure FRP bars, and a hybrid combination of steel and FRP bars.

Table 6(a) The details of the parametric study on the length of FRP bars

Parameter	Beam ID	Mz (mmxmm)*	f _c ' (MPa)	E _f (MPa)	f _f (MPa)	L _{FRP} (mm)*
Original beam	B4_FEM_Full	10x10	33.1	41000	755	Full
Length of FRP bars	B4_FEM_L1.2	10x10	33.1	41000	755	1200
	B4_FEM_L1.6	10x10	33.1	41000	755	1600

*Mz and L_{FRP}: The meshing element size of the FE models, and the length of FRP bar, respectively

Table 6(b) The details of the parametric study on concrete compressive strength and reinforcement ratios

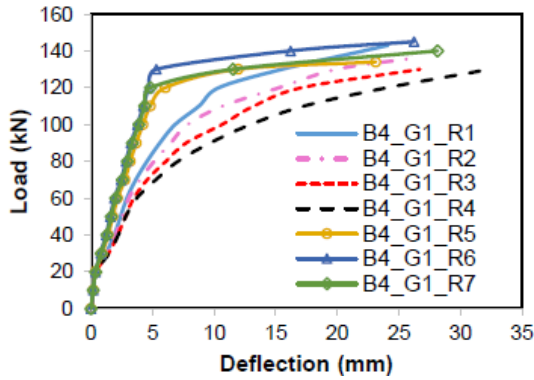
Group	Beam ID	A _s (mm ²)*	A _f (mm ²)*	ρ _r = A _f /A _s	f _f (MPa)	f _c ' (MPa)
Group 1	B4_G1_R1	200.96 (1d16)	628.32 (2d20)	3.127	755	33.1
	B4_G1_R2	200.96 (1d16)	508.94 (2d18)	2.533	755	
	B4_G1_R3	200.96 (1d16)	396.91 (2d15.9)	1.975	755	
	B4_G1_R4	200.96 (1d16)	307.88 (2d14)	1.532	755	
	B4_G1_R5	402.12 (2d16)	396.91 (2d15.9)	0.987	755	
	B4_G1_R6	508.94 (2d18)	307.88 (2d14)	0.605	755	
	B4_G1_R7	508.94 (2d18)	200.96 (1d16)	0.395	755	
Group 2	B4_G2_R1	200.96 (1d16)	628.32 (2d20)	3.127	755	44.5
	B4_G2_R2	200.96 (1d16)	508.94 (2d18)	2.533	755	
	B4_G2_R3	200.96 (1d16)	396.91 (2d15.9)	1.975	755	
	B4_G2_R4	200.96 (1d16)	307.88 (2d14)	1.532	755	
	B4_G2_R5	402.12 (2d16)	396.91 (2d15.9)	0.987	755	
	B4_G2_R6	508.94 (2d18)	307.88 (2d14)	0.605	755	
	B4_G2_R7	508.94 (2d18)	200.96 (1d16)	0.395	755	
Group 3	B4_G2_R1	200.96 (1d16)	628.32 (2d20)	3.127	755	60.0
	B4_G2_R2	200.96 (1d16)	508.94 (2d18)	2.533	755	
	B4_G2_R3	200.96 (1d16)	396.91 (2d15.9)	1.975	755	
	B4_G2_R4	200.96 (1d16)	307.88 (2d14)	1.532	755	
	B4_G2_R5	402.12 (2d16)	396.91 (2d15.9)	0.987	755	
	B4_G2_R6	508.94 (2d18)	307.88 (2d14)	0.605	755	
	B4_G2_R7	508.94 (2d18)	200.96 (1d16)	0.395	755	

*A_s and A_f: The area of the steel and GFRP tension reinforcement, respectively

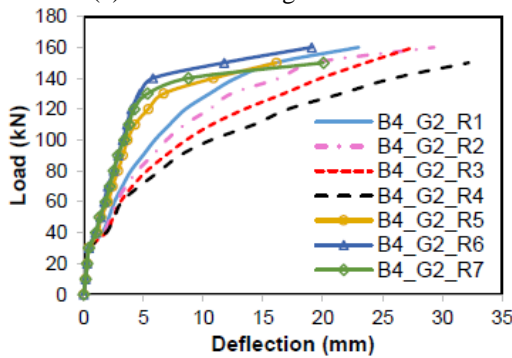
4. Parametric study by means of the finite element (FE) analysis

The reliability of FE simulations for the hybrid FRP-steel RC beams has been shown in Chapter 3. Besides, due to the simple geometry and reinforcement arrangement, the time for the FE analysis of the beam B4 is short. Thus, the developed FE model of a representative beam specimen B4 is easily employed to implement the parametric study.

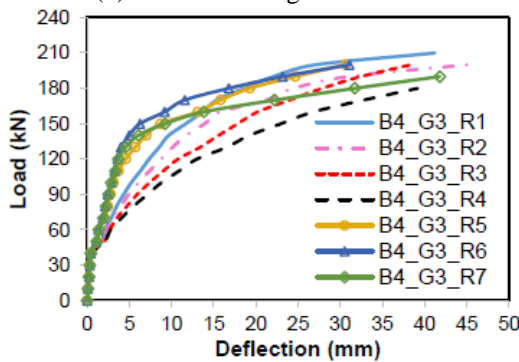
The specific parameters are as the concrete compressive strength, reinforcement ratios, the arrangement of tension reinforcement, and length of FRP bars. The change of concrete compressive strength with the values of 33.1 MPa, 44.5 MPa, and 60.0 MPa and the change of FRP and steel reinforcement ratios in the FE simulation of the beam B4 are investigated. For the effect of the length of FRP



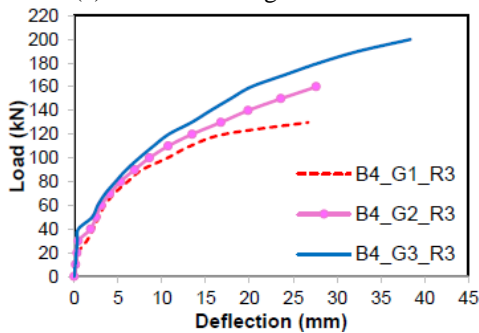
(a) Concrete strength 33.1 MPa



(b) Concrete strength 44.5 MPa



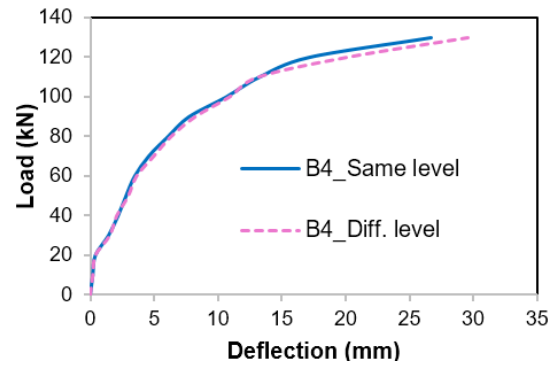
(c) Concrete strength 60.0 MPa



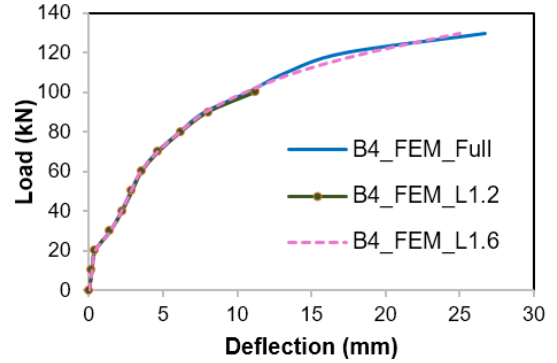
(d) Comparison in the effect of concrete strength

Fig. 10 Effects of concrete strength and reinforcement ratios on the response of the hybrid beams

bars on the response of the hybrid beam, the evaluation of the full length and the shorter length cases are carried out. To consider the effect of reinforcement arrangement, a FE model B4_Diff. level with the FRP bars in the outer layer of two layers of tension reinforcement is created to compare with the original one B4_Same level (FRP bars in one layer



(a) Effect of reinforcement positions



(b) Effect of length of FRP bars

Fig. 11 Effects of reinforcement positions and length of FRP bars on the response of the hybrid beams

of reinforcement) in Chapter 3. More details of the parametric study are described in Table 6(a) and Table 6(b).

For the effect of concrete compressive strength on the load-deflection response, ultimately applied load and midspan deflection results of the simulated hybrid beams are shown in Fig. 10 and Table 7. In Fig. 10(d), by considering a representative beam of B4 in the three groups at Table 6(b), as expected the B4_G3_R3 and B4_G2_R3 models achieve the higher load-carrying capacities than that of the control beam B4_G1_R3 by 53.85% and 23.08%, respectively. Additionally, the increase of 3.37% and 43.82% in the midspan displacements are calculated for the corresponding beams B4_G2_R3 and B4_G3_R3 in the comparison with the reference specimen B4_G1_R3.

In Fig. 10, there is a clear correlation between the load-deflection performance and the reinforcement ratio. With the increase of FRP reinforcement content, the load carrying capacity increases and the displacement decreases. Besides, it is obvious that the stiffness of hybrid FRP-steel RC beam is governed by the reinforcement ratio of A_f/A_s . The lower hybrid reinforcement ratios A_f/A_s result in the higher stiffness, which are clearly shown in the Figs. 10(a)-(c). However, this correlation is different in the case of $A_f/A_s > 1$, since this case used the same content of steel reinforcement. Therefore, the stiffness enhances by increasing the FRP content. The influences of the concrete compressive strength and reinforcement ratio on the ductility of concrete beam reinforced by FRP and steel bars are deeply discussed in section 5.5 of Chapter 5.

The behavior of the two concrete beams reinforced with the different positions of FRP and steel bars are performed

Table 7 Effects of concrete compressive strength, reinforcement arrangement, and length of FRP bars

Parameter	Specimen	Failure load (kN)	Difference in load (%)	Failure deflection (mm)	Difference in deflection (%)
Concrete strength	B4_G1_R3	130	NA	26.7	NA
	B4_G2_R3	160	23.08	27.6	3.37
	B4_G3_R3	200	53.85	38.4	43.82
Reinforcement arrangement	B4_Same level	130	NA	26.7	NA
	B4_Diff. level	130	0.00	29.6	10.86
Length of FRP bars	B4_FEM_Full	130	NA	26.7	NA
	B4_FRP_L1.2	100	-23.08	11.2	-58.05
	B4_FRP_L1.6	130	0.00	25.0	-6.37

in Fig. 11(a). It is obvious that the response in service conditions, 60% of the ultimate load, of the two specimens B4_Same level and B4_Diff. level is similar, however, the slope of load-deflection curves of those beams is changed at high load level. Specifically, the stiffness of the specimen B4_Same level is higher than that of the specimen B4_Diff. level. Furthermore, Table 7 shows the load-carrying capacity of beam reinforced by the different level of tension bars is similar to that of the concrete member with the same level of GFRP and steel reinforcement. However, the maximum deflection of the hybrid beam with the two layers of bars is increased by 10.86% in the evaluation with the similar component reinforced by one layer of bars. Thus, placing the different level of steel and FRP bars would ensure the rigidity of the hybrid beams. For the prevention of corrosion of steel reinforcement, FRP bars are placed in the outer layer and steel bars are laid in the inner layer.

Fig. 11(b) shows the effect of FRP length on the predicted load-displacement response of concrete beams reinforced by FRP and steel bars. Specimen B4_FEM_L1.2 with a FRP length of 1.2 m indicates a significant decrease of deflection and strength in the comparison with concrete beam reinforced by full-length FRP bars, and the specific reductions are implied in Table 7 by dropping 23.08% and 58.05% in the load-carrying capacity and midspan displacement, respectively. The reason is concrete crushing at section where FRP reinforcement is ended. Whereas employing the FRP bars with the length of 1.6 m to reinforce concrete beam (B4_FEM_L1.6), the ultimate load and deflection are insignificantly varied via the comparison with the control specimen (B4_FEM_Full). The 0.00% is represented by the deviation in the ultimate load capacity of the two beams have just mentioned. In addition, the maximum deflection of B4_FEM_L1.6 is lower than that of specimen B4_FEM_Full about 6.37%.

5. Design models

This Chapter shows the design models of hybrid FRP-steel RC beams in the literature. The comparison and verification with the experimental results are carried out. Besides, the new approach for evaluating the deflection and ductility of concrete beams with the hybrid usage of steel and FRP reinforcement are also proposed. The following

Table 8 A comparison of tested and analytical results in the moment capacity

Study	Beam ID	$M_{n,e}$ (kNm)	$M_{n,a}$ (kNm) Eq. (2)	Difference (%)
Aiello and Ombres (2002)	A1	25.1	23.6	5.98
	A2	28.4	31.4	10.56
	A3	35.6	44.6	25.28
	B3	38.3	36.2	5.48
	B4	39.7	38.4	3.27
	B5	36.4	36.1	0.82
	B6	42.6	41.9	1.64
	B7	23.6	27.2	15.25
Qu <i>et al.</i> (2009)	B8	63.3	66.4	4.90
	G0.6-T1.0-A90	229	251.0	9.61
	Lau and Pam (2010) G1.0-T0.7-A90	261	265.0	1.53
	G0.3-MD1.0-A90	147	149.4	1.63

 Table 9 Equations of effective moment of inertia (I_e)

Authors	Effective moment of inertia (I_e)	Remarks
ACI 440R-96 (ACI 1996b)	$I_e = \beta I_s \left(\frac{M_{cr}}{M_{max}} \right)^3 + I_{cr} \left[1 - \left(\frac{M_{cr}}{M_{max}} \right)^3 \right]$	$\beta = \alpha \left(\frac{E_{FRP}}{E_{steel}} + 1 \right), \alpha = 0.5$
Aiello and Ombres (2002)	$I_e = \alpha_{cal} I_s \left(\frac{M_{cr}}{M_{max}} \right)^3 + \beta_{cal} I_{cr} \left[1 - \left(\frac{M_{cr}}{M_{max}} \right)^3 \right]$	$\alpha_{cal}, \beta_{cal}$ obtained from calibration of tested results $I_s = bh^3/12, M_{cr} = 2f_t I_s / h$ $f_t = 0.62\sqrt{f_c}$ $I_e = \frac{1}{3}bd^3k^3 + (n_s A_s + n_f A_f) d^3 (1-k)^3$ $k = \sqrt{(\rho')^2 + 2\rho' - \rho'}$ $\rho' = n_s \rho_s + n_f \rho_f$
Bischoff (2007)	$I_e = \frac{I_{cr}}{1 - \eta \left(\frac{M_{cr}}{M_{max}} \right)^2}$	$\eta = 1 - \frac{I_{cr}}{I_s}$

sections present the determination of the flexural strength, the deflection prediction, crack width, and ductility analysis.

5.1 Ultimate flexural moment

Qu *et al.* (2009) offered a theoretical equation to compute the moment capacity of concrete beams with the combination of FRP and steel bars. The model of the flexural moment was based on the force equilibrium, strain compatibility and ACI rectangular stress block hypothesis for the stress distribution in compressive concrete (Qu *et al.* 2009). And it should be noted that the method to build this model is very similar to the technique to determine the moment capacity of steel reinforced concrete beams. The flexural moment of hybrid FRP and steel RC beams could be calculated by using Eq. (2).

$$M_n = (\rho_f f_f + \rho_s f_y) \left(1 - 0.59 \frac{\rho_f f_f + \rho_s f_y}{f_c} \right) b d^2 \quad (2)$$

The comparison of experimental and analytical results in the flexural moment capacity of hybrid beams is shown in Table 8. And the maximum difference of the flexural strengths in the comparison between tested and theoretical results is 25.28%. Therefore, it is apparent that the model of Qu *et al.* (2009) could be employed to determine the moment capacity of concrete beams reinforced with FRP and steel bars. Note that d (mm) = section effective depth.

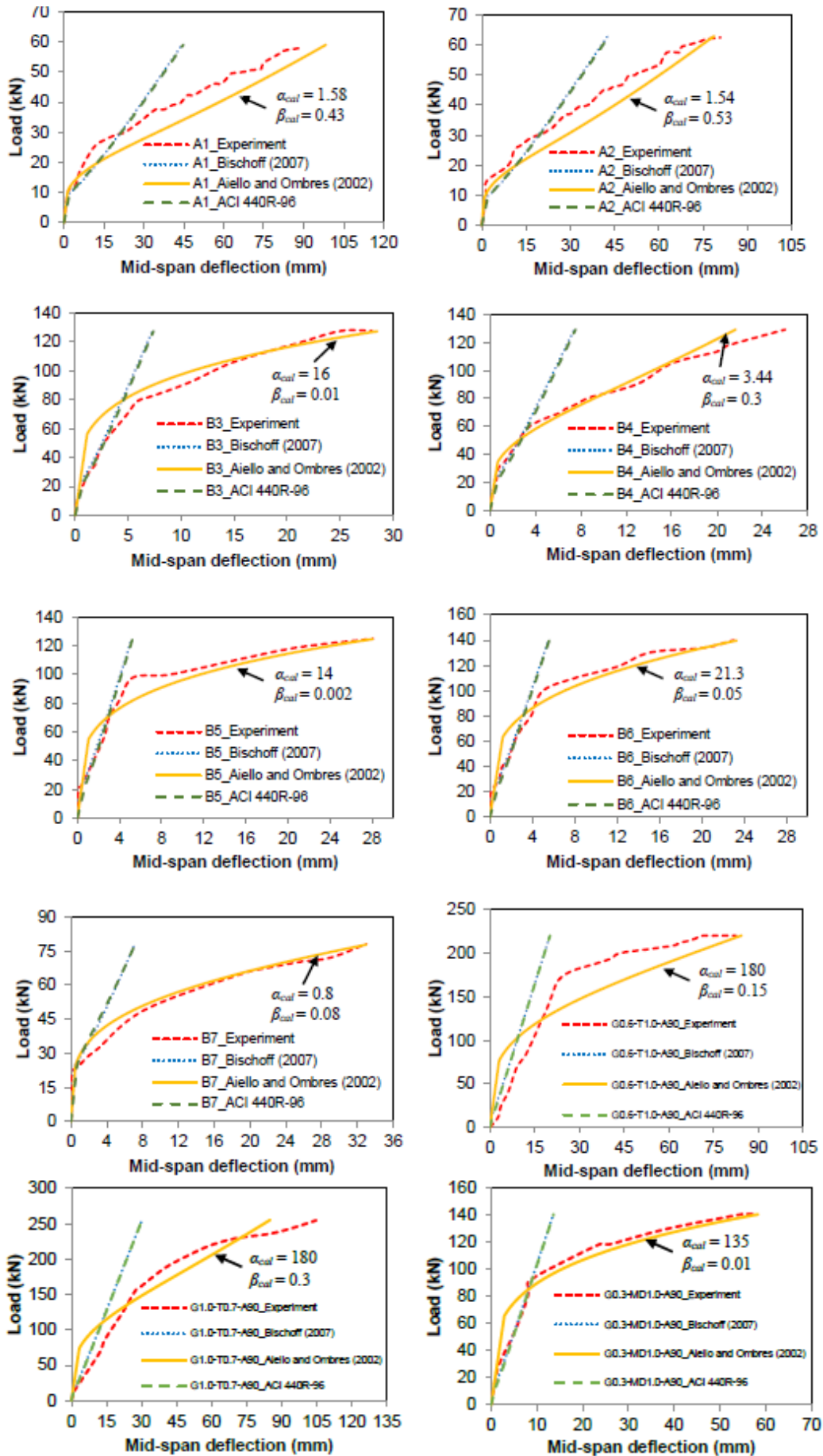


Fig. 12 Experimental and analytical deflection of hybrid beams

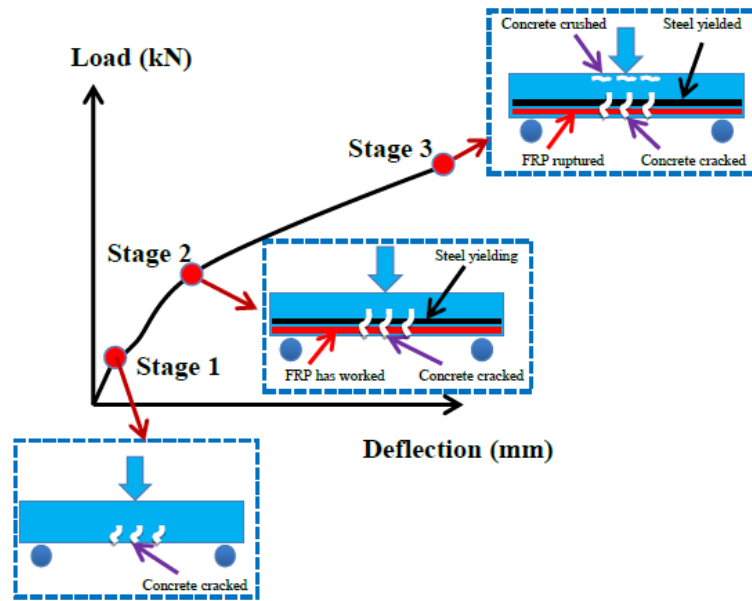


Fig. 13 General behavior of hybrid beams

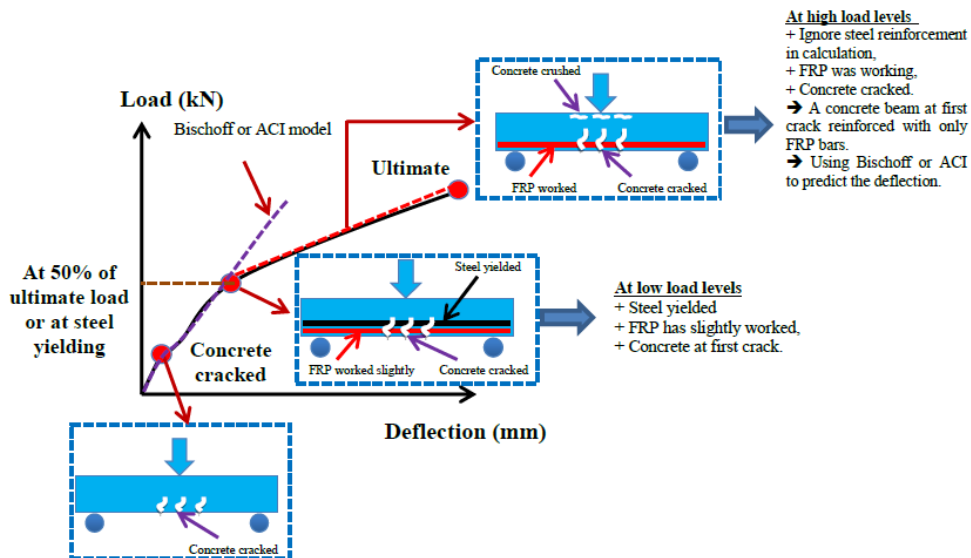


Fig. 14 Assumption of developed model

5.2 The current equations of deflection calculation

There were three common formulations to evaluate the deflection of hybrid beams based on the models of Branson (1977) and Bischoff (2007). These equations were using the effective moment of inertia (I_e) in combination with elastic deflection formulas to determine the deflection of concrete beams reinforced by FRP and steel bars. The formulas of the effective moment of inertia are summarized in Table 9.

Where I_{cr} (mm^4) = moment of inertia of transformed crack section; I_g = gross moment of inertia; M_{cr} (kNm) = cracking moment; f_{cr} (MPa) = modulus of rupture of concrete; M_{max} (kNm) = maximum moment in the member at the current phase of deflection; h (mm) = overall height of concrete beam; n_f ($= E_f/E_c$) = elastic modulus ratio between FRP reinforcement and concrete; n_s ($= E_s/E_c$) = elastic modulus ratio between steel reinforcement and

concrete; and d (mm) = distance from extreme compression fiber to the centroid of the tension reinforcing zone (effective depth).

Qu *et al.* (2009) suggested that the short-term deflection of a simply supported beam under four-point loading were computed by Eq. (3).

$$\Delta = \frac{23}{1296} \frac{Pl^3}{E_c I_e} \quad (3)$$

And the deflection of simple beams with three-point loading could be defined as Eq. (4).

$$\Delta = \frac{1}{48} \frac{Pl^3}{E_c I_e} \quad (4)$$

Where P (kN) = midspan applied load; l (mm) = span

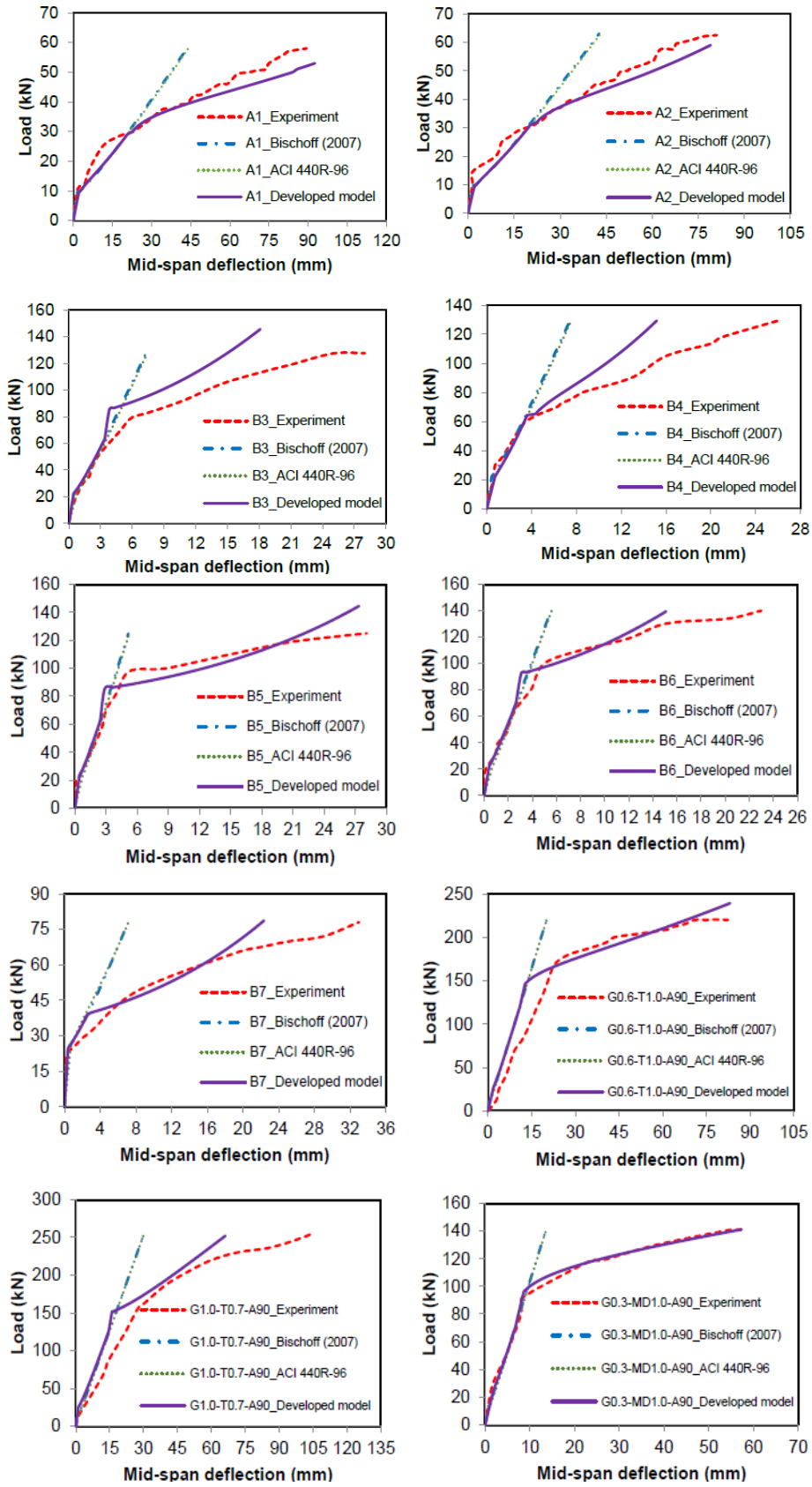


Fig. 15 Tested and theoretical deflection of hybrid beams

length; E_c (MPa) = elastic modulus of concrete; and I_e (mm^4) = effective moment of inertia was computed by using the equation in Table 9.

Fig. 12 shows the comparison between the experimental and analytical results in terms of load-midspan deflection curves of the hybrid beams tested by Aiello and Ombres

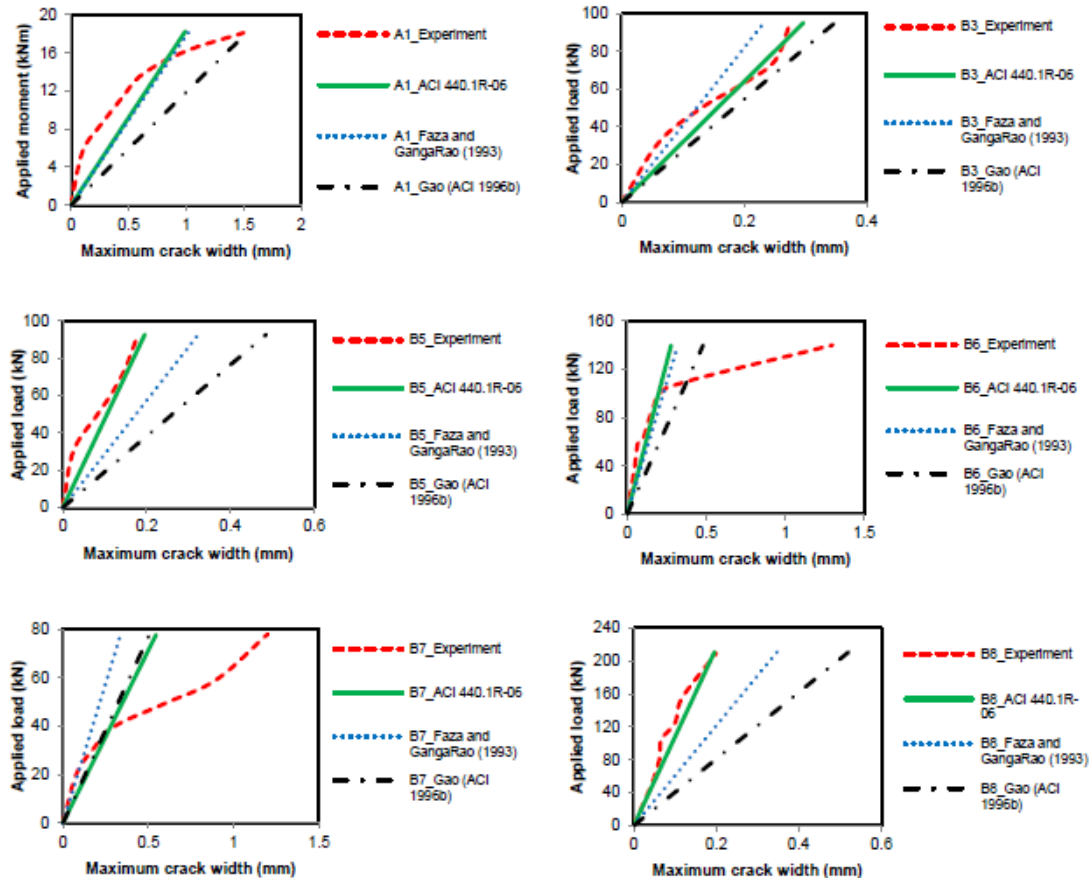


Fig. 16 The predicted and experimental maximum crack width

(2002), Qu *et al.* (2009), Lau and Pam (2010). The deflection models of Bischoff (2007), ACI 440R-96, and Aiello and Ombres (2002) are adopted to compute and discuss.

The models of ACI 440R-96 and Bischoff (2007) perform the similar curves in all beam specimens and fit well with experimental results at low load levels (lower than 50% of the ultimate load). For high load levels, the results attained by using the equations of Bischoff (2007) and ACI 440R-96 are significantly underestimated in the comparison with the experimental data. Whereas, predictions found by means of Aiello and Ombres (2002)'s model are close to the tested results for concrete beams reinforced with the combination of FRP and steel bars. However, the equation of Aiello and Ombres (2002) is calibrated from experimental data via the coefficients of α_{cal} , β_{cal} . Therefore, a new model is expected to improve the prediction of load-midspan displacement response for hybrid FRP-steel RC beams.

5.3 Developed model for deflection prediction

The general behavior of concrete beams with the hybrid usage of FRP and steel reinforcement is shown in Fig. 13. At first stage, tensile concrete is cracked, the steel and FRP reinforcement are beginning to activate under the increase of the applied load. Then, the concrete cracking zone propagates vertically and then horizontally to the two ends

of beams. Until the steel reinforcement yields, FRP reinforcement slightly works. This is the behavior of hybrid FRP-steel RC beams at the end of stage 2. At the remaining stage in which the steel reinforcement yields, FRP is significantly activated, and concrete is crushed in compression zone resulting in the failure of the hybrid beam.

Fig. 14 shows the hypothesis for the new approach to determine the deflection of concrete beams reinforced by FRP and steel bars. Section 5.2 revealed that the equations of Bischoff (2007) and ACI 440R-96 could predict the deflection of hybrid beams at low load levels (lower than 50% of the ultimate load and before steel yielding). The assumptions for the improved model are the steel reinforcement is yielded at either 50% of the ultimate load point or steel yielding point. In addition, the concrete is still maintained at first crack, and FRP bar has slightly worked at low load levels.

For high load levels (after steel yielding), the FRP reinforcement is being tensioned and concrete cracks are opening and propagating till the beam is failed. The developed model emphasizes that in the calculation of increment of deflection at high load levels, the hybrid beam is considered as a concrete beam at first crack reinforced in tension with solely FRP bars. Besides, the applied load is started from the load level caused the first crack for the hybrid beams. After yielding of steel reinforcement, the increment of deflection is calculated by either Bischoff

Table 10 Crack width prediction of hybrid FRP-steel RC beams

Authors	Crack width equations	Remarks
Faza and GangaRao (1993)	$w = 0.0112\beta_1 \frac{E_s}{E_f} f_{FRP} \sqrt[3]{d_c A} \times 10^{-3}$	$\beta_1 = \beta_2 - 1$
ACI 440R-96	$w = 0.0112\beta_1 k_f f_{FRP} \sqrt[3]{d_c A} \times 10^{-3}$	$\beta_1 = \beta_2 - 1, k_f = k_b E_s / E_f$
ACI 440.1R-06	$w = 2\varepsilon_f \beta_2 k_b \sqrt{d_c^2 + (s/2)^2}$	$\varepsilon_f = \frac{M_u}{(A_s E_s + A_f E_f) d (1-k/3)}, \beta_2 = \frac{h-kd}{d(1-k)}$

(2007) or ACI 440R-96 without considering the steel reinforcement contribution. The total load-deflection graphs of the hybrid FRP-steel RC beams are combined by the two curves of the low and high load stages.

The verifications of the tested results with the predicted results computed according to the proposed model and the equations of Bischoff (2007), ACI 440R-96 for the beams A1, A2, B3, B4, B5, B6, B7, G0.6-T1.0-A90, G1.0-T0.7-A90, G0.3-MD1.0-A90 are investigated and shown in Fig. 15. It is obvious from Fig. 15 that the response of developed model results is in far better agreement with the tested data rather than the results obtained from the models of Bischoff (2007) and ACI 440R-96. The new model indicates a good prediction not only at low load levels but also at high load levels. Moreover, the correlation between the reinforcement ratio (A_f/A_s) of the collected specimens in Tables 1-2-3 and the results performed in Fig. 15 is carefully observed. In general, the recommended model compares well with the experimental data at low and medium A_f/A_s ratios. From the aforementioned assessments, the model improved in this study could be employed to predict the load-deflection relationship of concrete beams reinforced by FRP and steel bars with reasonable precision and simple application. To extend this topic, the reduction factors for concrete, steel, and FRP materials at high load stage can be added into the developed model to achieve the better expectations.

5.4 Crack width

Faza and GangaRao (1993), ACI 440R-96 (Gao (ACI-1996b)), and ACI 440.1R-06 suggested the formulations for evaluating the crack width of concrete beams reinforced with FRP and steel bars, and the equations of the current models are listed in Table 10. Moreover, the comparison between the experimental data and the numerical results calculated according to the previously described study and code equations are also implemented.

Where A (mm^2) = effective tension area of rebar; β_1 = ratio of the distance between the reinforcement centroid and the tension fiber to the distance between the reinforcement centroid and the neutral axis; f_{FRP} (MPa) = stress in FRP reinforcement at load stage; d_c (mm) = thickness of the concrete cover to the center of closest bar; k_f = modification coefficient considers the response of FRP bars; k_b = bond properties of bars, for models of Faza and GangaRao (1993), Gao (ACI 1996b) $k_b = 1.5$, and for model of ACI 440.1R-06 $k_b = 1.0$ for steel, 1.4 for FRP, and 1.4 for hybrid steel-FRP reinforcement; s (mm) = longitudinal bar spacing. Fig. 16 presents the plot of the maximum crack width versus the applied moment and load by taking into account

Table 11 Ductility indices of the experimental results

Authors	Beam ID	DF	u_u/u_y	u_u/l	μ_h	Current study $(\Delta u_x F_u)/(\Delta F_x u_u)$
	A1	7.95	6.92	1/30	5.41	1.56
Aiello and Ombres (2002)	A2	6.27	6.08	1/34	4.01	1.70
	A3	4.16	4.08	1/17	3.04	2.29
	B3	5.03	4.78	1/65	3.52	2.15
	B4	5.00	8.42	1/69	3.20	1.73
Qu <i>et al.</i> (2009)	B5	5.20	5.87	1/62	4.42	2.98
	B6	4.37	4.82	1/75	3.41	2.80
	B7	9.32	11.00	1/41	5.87	1.65
	B8	1.75	1.61	1/127	1.70	0.53
	G0.6-T1.0-A90	2.84	4.19	1/40	2.47	1.89
Lau and Pam (2010)	G1.0-T0.7-A90	3.07	3.86	1/39	2.61	1.90
	G0.3-MD1.0-A90	7.06	7.28	1/66	5.86	1.99

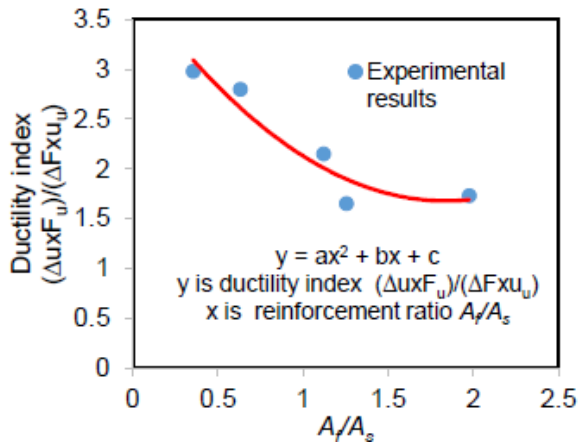
the experimental and analytical results. The hybrid FRP-steel beams of A1, B3, B5, B6, B7, and B8 are considered and discussed. By comparing with the tested data, the results obtained from the maximum crack width equation of ACI 440.1R-06 is more accurate than the results attained by applying the models of Faza and GangaRao (1993) and ACI 440R-96. Therefore, it is clearly implied that the formulation of ACI 440.1R-06 could be adopted to compute the maximum crack width of concrete beams with a hybrid combination of FRP and steel reinforcement. Generally, all of the formulas furnish a good evaluation at low values of applied loads, whereas the crack widths calculation is dramatically different for high load levels. Since the bond effect (k_b) of FRP and concrete influenced strongly on the computed results.

5.5 Ductility analysis

Pang *et al.* (2015) reviewed the ductility indices in the works of Tan (1997), Aiello and Ombres (2002), and Lau and Pam (2010). A new ductility model was also recommended for hybrid RC beams by Pang *et al.* (2015). The current study proposes a simple ductility index to evaluate the ductility of hybrid FRP-steel RC beams based on the response of the beams after steel yielding. The data in the research of Pang *et al.* (2015) is also mentioned to discuss and confirm with the new model.

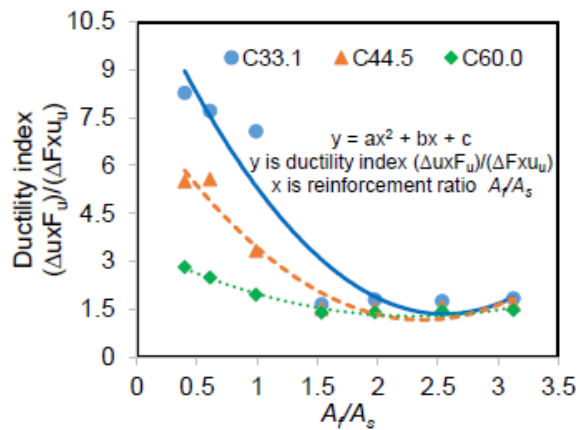
Fig. 13 indicated that the behavior of concrete beams reinforced by FRP-steel bars was divided into the three stages. In order to consider the ductility of the beams, stage 2 and stage 3 are conservatively investigated. This research focuses on the ratio of the deflection and applied load after the steel yielding for the ductility evaluation. The ratio of $(\Delta u_x F_u)/(\Delta F_x u_u)$ is used to evaluate the ductility of concrete beams with the hybrid usage of steel and FRP reinforcement. Where $\Delta u = u_u - u_y$ (mm), $\Delta F = F_u - F_y$ (kN), and F_u, F_y, u_u, u_y are corresponding for the applied loads and deflections at the ultimate, steel yielding.

Table 11 shows the results of ductility of the hybrid FRP-steel RC beams in the literature calculated according



Regression	a	b	c	R ²
Tested data	0.64	-2.36	3.85	0.912

Fig. 17 Relationship of reinforcement ratio and ductility index in the beams (B1-B7) of Qu *et al.* (2009)



Regression	a	b	c	R ²
C33.1	1.63	-8.35	12.01	0.908
C44.5	1.20	-5.68	7.91	0.952
C60.0	0.41	-1.89	3.46	0.975

Fig. 18 Relationship of reinforcement ratio and ductility index in the beams of parametric study

to the methods of the Aiello and Ombres (2002), Lau and Pam (2010), conventional steel RC beams, Pang *et al.* (2015), and the proposed technique. The model of Aiello and Ombres (2002) was based upon the deformability factor (*DF*), which referred the research of Vijay and GangaRao (1996), defined as the ratio of the energy absorption at ultimate to the energy computed with respect to a limiting curvature. Lau and Pam (2010) suggested the ductility index was the ratio of the ultimate deflection and span length of the hybrid beams (u_u/l). While the ratio of the ultimate and yield displacement (u_u/u_y) was used for the ductility analysis in the conventional steel RC beams. The index μ_h was explored to investigate the ductility of the hybrid beams in the study of Pang *et al.* (2015). More details of the ductility analysis were reported and could be found in the references.

From Table 11, a similar trend of ductility indices is observed in the studies of Qu *et al.* (2009), and Lau and

Pam (2010) by means of the current work and Pang *et al.* (2015). Table 11 implies that beam B8 is the most brittle because of the smallest values of μ_h and $(\Delta u_x F_u)/(\Delta F_x u_u)$. Hence, beam B8 is immediately failed after steel yielding and this is also suitable for the actual response of the tested results. For the beams A1, A2, and A3, the proposed ductility ratio provides the same ranking with the model of Lau and Pam (2010). It is obvious that beam A3 has the largest values of $(\Delta u_x F_u)/(\Delta F_x u_u)$ and u_u/l , thus the most ductile beam is A3, however, the stiffness of this beam is significantly reduced due to the high value of $(\Delta u_x F_u)/(\Delta F_x u_u)$. The ductility evaluations by adopting the new method as well as the models of Lau and Pam (2010) and Pang *et al.* (2015) are slightly different in the comparison with the ductility assessments using formulas of Aiello and Ombres (2002) and the conventional steel RC beams.

Fig. 17 demonstrates a relationship of reinforcement ratio A_f/A_s and ductility index $(\Delta u_x F_u)/(\Delta F_x u_u)$ of the hybrid beams B1-B7 in the study of Qu *et al.* (2009). It is clearly indicated that the ductility index increases when the hybrid reinforcement ratio decreases and a second order polynomial regressive equation is performed for curve-fitting the experimental data. Additionally, an extensive consideration for the ductility of the hybrid FRP-steel RC beams using the parametric study in Chapter 4 is carried out. The simulated results from Figs. 10(a)-(c) of the three groups of beams with the difference of concrete compressive strength and reinforcement ratio in Table 6(b) are employed to investigate the ductility of concrete beams reinforced by FRP and steel bars. Fig. 18 reveals the relationship between ductility index and reinforcement ratio of the simulated beams in the parametric study.

The similar trends are found in Fig. 18 and the tested data in Fig. 17, decreasing the hybrid reinforcement ratio A_f/A_s , the ductility index $(\Delta u_x F_u)/(\Delta F_x u_u)$ enhances. After taking the regression of the data, the second order polynomial equation is acceptable to perform the ductility index by the reinforcement ratio. In addition, it is obvious from Fig. 18 that the ductility ratio reduces by increasing the concrete compressive strength. This correlation is explicit for the case of low hybrid reinforcement ratio. By contrast, the influence of concrete strength on ductility index is not significant at high and medium A_f/A_s ratios. Moreover, the ductility requirement of $(\Delta u_x F_u)/(\Delta F_x u_u)$ should be not less than 1.4 is easily satisfied with a concrete compressive ranging from 33.1 to 60.0 MPa. In addition, this study recommends that the reinforcement ratio A_f/A_s should be 1 around to ensure the ductility and stiffness of concrete beams reinforced with FRP and steel bars. Summarily, the indices of Lau and Pam (2010), Pang *et al.* (2015), and the current research could be employed to evaluate the ductility of the hybrid FRP-steel beams. Besides, the authors believe that the further discussion on this topic is needed.

6. Conclusions

This study gained insight into the mechanical performances of FRP-steel hybrid RC beams by discovering

many previous studies. Finite element analyses were implemented to simulate the nonlinear behavior of concrete beams with the hybrid usage of steel and FRP reinforcement. This research carried out the parametric study for the hybrid FRP-steel RC beams by means of the finite element program. Moreover, the discussions on the design models were also considered and evaluated. From the investigated numerical and analytical results, the following conclusions can be drawn:

- The reliable FE models were built to obtain the good predictions for the response of the steel RC beams, FRP RC beams, and hybrid FRP-steel beams with reasonable accuracy in the comparison with the tested results.

- For the parametric study, the effects of the hybrid reinforcement ratio, concrete compressive strength, arrangement of tension reinforcement, and length of FRP bars influenced dramatically on the structural behavior of concrete beams reinforced with FRP and steel bars. Those parameters are desirable to investigate by conducting an experimental program in the future research.

- The equation of Qu *et al.* (2009) for calculating the moment capacity compared well with the tested data by the maximum difference was 25.28%. Therefore, the model of Qu *et al.* (2009) could be totally used to calculate the ultimate moment capacity of the hybrid FRP-steel RC beams.

- An effective and simple design model was developed for predicting the load-deflection relationship of concrete beams with the combination of FRP and steel bars. By comparing with experimental data, the precision of the results attained from the improved model was significantly higher than the one obtained by the existing methods.

- At present, the ACI 440.1R-06 was a favorable formula to compute the maximum crack width of the hybrid FRP-steel RC beams. However, the equation of ACI 440.1R-06 has just performed a good agreement with the experimental results at low load levels. Therefore, a better model for determining the crack width of concrete beams reinforced by FRP and steel bars should be suggested.

- This research provided the useful database to consider the ductility of the hybrid beams. In addition, a simple ductility index was proposed to evaluate the ductility and stiffness of concrete beams reinforced with steel and FRP bars. The recommended model indicated the good agreements with the indices of Lau and Pam (2010), and Pang *et al.* (2015) in the ductility evaluation. A concrete member was considered as a ductile and stiff beam when the ductility ratio $(\Delta u_x F_u)/(\Delta F_x u_u)$ is greater than 1.4 for the range of concrete strength from 33.1 to 60 MPa and reinforcement ratio A_f/A_s from 0.395 to 3.127. Additionally, this paper suggested the hybrid reinforcement ratio should be 1 around to maintain the ductility and stiffness of concrete beams with the combination of steel and FRP bars.

Acknowledgments

The authors acknowledge the financial support of the ASEAN University Network/Southeast Asia Engineering Education Development Network-AUN/SEED-Net.

References

- ACI 440.1R-06 (2006), *Guide for the Design and Construction of Structural Concrete Reinforced with FRP Bars*, American Concrete Institute, Detroit, U.S.A.
- ACI 440R-96 (1996b), *State of the Art Report on Fiber Reinforced Plastic Reinforcement for Concrete Structures*, American Concrete Institute, Detroit, U.S.A.
- Aiello, M.A. and Ombres, L. (2002), "Structural performances of concrete beams with hybrid (fiber-reinforced polymer-steel) reinforcements", *J. Compos. Constr.*, **6**(2), 133-140.
- ANSYS-Release Version 15.0 (2013), *A Finite Element Computer Software and User Manual for Nonlinear Structural Analysis*, Canonsburg, U.S.A.
- Bencardino, F., Condello, A. and Ombres L. (2016), "Numerical and analytical modeling of concrete beams with steel, FRP and hybrid FRP-steel reinforcements", *Compos. Struct.*, **140**, 53-65.
- Bischoff, P.H. (2007), "Deflection calculation of FRP reinforced concrete beams based on modifications to the existing Branson equation", *J. Compos. Constr.*, **11**(1), 4-14.
- Branson, D.E. (1977), *Deformation of Concrete Structures*, McGraw-Hill, New York, U.S.A.
- Faza, S.S. and GangaRao, H.V.S. (1993), *Theoretical and Experimental Correlation of Behaviour of Concrete Beams Reinforced with Fiber Plastic Rebars*, Fiber Reinforced Plastic Reinforcement for Concrete Structures, SP-138, American Concrete Institute, Detroit, U.S.A.
- Ge, W., Zhang, J., Cao, D. and Tu, Y. (2015), "Flexural behaviors of hybrid concrete beams reinforced with BFRP bars and steel bars", *Constr. Build. Mater.*, **87**, 28-37.
- Godat, A., Labossière, P., Neale, K.W. and Chaallal, O. (2012), "Behavior of RC members strengthened in shear with EB FRP: Assessment of models and FE simulation approaches", *Comput. Struct.*, **92-93**, 269-282.
- Hawileh, R.A. (2015), "Finite element modeling of reinforced concrete beams with a hybrid combination of steel and aramid reinforcement", *Mater. Des.*, **65**, 831-839.
- Hind, M.K., Mustafa, O., Talha, E. and Abdolbaqi, M.K. (2016), "Flexural behavior of concrete beams reinforced with different types of fibers", *Comput. Concrete*, **18**(5), 999-1018.
- Hognestad, E., Hanson, N.W. and McHenry, D. (1955), "Concrete stress distribution in ultimate strength design", *ACI J. Proc.*, **52**(12), 455-479.
- Kara, I.F., Ashour, A.F. and Köroğlu, M.A. (2015), "Flexural behavior of hybrid FRP/steel reinforced concrete beams", *Compos. Struct.*, **129**, 111-121.
- Kara, I.F. (2016), "Flexural performance of FRP-reinforced concrete encased steel composite beams", *Struct. Eng. Mech.*, **59**(4), 775-793.
- Lau, D. and Pam, H.J. (2010), "Experimental study of hybrid FRP reinforced concrete beams", *Eng. Struct.*, **32**(12), 3857-3865.
- Oller, E., Marí, A., Bairán, J.A. and Cladera, A. (2015), "Shear design of reinforced concrete beams with FRP longitudinal and transverse reinforcement", *Compos. Part B: Eng.*, **74**, 104-122.
- Pang, L., Qu, P., Zhu, P. and Xu, J. (2015), "Design propositions for hybrid FRP-steel reinforced concrete beams", *J. Compos. Constr.*, **20**(4), 1-9.
- Qin, R., Zhou, A. and Lau, D. (2017), "Effect of reinforcement ratio on the flexural performance of hybrid FRP reinforced concrete beams", *Compos. Part B: Eng.*, **108**, 200-209.
- Qu, W., Zhang, X. and Huang, H. (2009), "Flexural behavior of concrete beams reinforced with hybrid (GFRP and steel) bars", *J. Compos. Constr.*, **13**(5), 350-359.
- Tan, K.H. (1997), "Behavior of hybrid FRP-steel reinforced concrete beams", *Proceedings of the 3rd International Symposium on Non-Metallic (FRP) Reinforcement for Concrete*

- Structures (FRPRCS-3)*, Japan Concrete Institute, Tokyo, 487-494.
- Vijay, P.V. and GangaRao, H.V.S. (1996), "A unified limit state approach using deformability factors in concrete beams reinforced with GFRP bars", *Proceedings of the 4th Conference on Materials Conference, Materials for The New Millennium*.
- Yoo, D.Y. and Banthia, N. (2015), "Numerical simulation on structural behavior of UHPFRC beams with steel and GFRP bars", *Comput. Concrete*, **16**(5), 759-774.
- Yoo, D.Y., Banthia, N. and Yoon, Y.S. (2016), "Flexural behavior of ultra-high-performance fiber-reinforced concrete beams reinforced with GFRP and steel rebars", *Eng. Struct.*, **111**, 246-262.
- Zhang, D., Wang, Q. and Dong, J. (2016), "Simulation study on CFRP strengthened reinforced concrete beam under four-point bending", *Comput. Concrete*, **17**(3), 407-421.

HK